

Cell Fusion Generates an Inhomogeneous Distribution of Elasticity and Rigidity in Plasma Membranes

M. Baumann

Institute of Physiology, RWTH Aachen, Pauwelsstr. 30, 52057 Aachen, Germany

Received: 19 August 2001/Revised: 4 January 2002

Abstract. The post-electrofusion oscillation cycle of human erythrocytes (doublets) was evaluated for the first four pump events in order to quantify the spectrin-network rearrangement in the fusion zone. Experiments were carried out on control cells and on cells that received a 40°C and a 45°C 20-min heat treatment. The amplitude of the geometrical changes depended on the heat-treatment procedure, whereas the roundness on entering the pump event was always identical. The rigid influence of the fusion zone prevented the doublets from adopting a spherical shape. The fusion zone was characterized by a linear elongation modulus that could be calculated from geometrical measurements and earlier findings on erythrocyte membrane mechanics, and that ranged between $1.44\text{E}6 \text{ Nm}^{-2}$ for control doublets and $0.99\text{E}6 \text{ Nm}^{-2}$ after 45°C heat treatment. The membrane composition of the fusion zone differs greatly from that of the other membrane parts not involved in fusion processes and evidence is given that this inhomogeneity stems from a rearrangement of the triangulated spectrin network and other membrane skeletal proteins in the fusion zone.

Key words: Erythrocyte — Membrane — Electrofusion — Postfusion oscillation — Spectrin — Fusionzone — Elongation modulus

Introduction

Cell and membrane fusion is essential for numerous physiological processes like stem cell division, growth, endo- and exocytosis in digestion and synaptic signalling, blood cell genesis, immune defense and lots of others. The term “cell fusion” itself denotes a multi-stage process exhibiting a sequence of

consecutive steps starting with physical membrane contact, followed by bilayer joining or hemifusion [21, 35], membrane fission and open lumen fusion [37], which is driven [1] and/or controlled [29] by colloidosmotic forces and results in a topological and functional syncytium [37]. Changes of the osmolarity also have an effect on the regulation of the actin cytoskeleton [18].

A good paradigm cell to do fusion kinetics research with is the erythrocyte, which, due to the lack of organelles, adopts its static shape and dynamic behavior as a consequence of membrane mechanics only [31, 32]. As lipid bilayer and associated membrane-macromolecule composition is comparable to nucleated cells [9], and as the erythrocyte can be obtained very easily in always sufficient amounts, this cell type serves as an excellent model for procedures that are affected by and involve membrane mechanics. The objective of this study is to characterize the membrane area in the fusion zone itself and to give new and strong evidence that its altered mechanical properties are due to the rearrangement of the membrane-associated spectrin molecules. Fusion can be initiated chemically [22, 28], in the presence of viruses [22, 26, 36] or proteins [13], with laser light [40] and electrically [45]. The latter one is often used due to its independence of the target cell type, its transient effect, the possibility to trigger experimental data acquisition apparatus [36], and its well-defined and short-term impact. Fusion kinetics of a cell-to-cell fusion product (a doublet) are characterized with low-speed [14] or high-speed [3] videorecording and measurement of various geometrical parameters such as the timeline of the fusion zone diameter (FZD) alone [38], and/or the timelines of the radii of the fused spheres [3].

The influence of spectrin molecules and other membrane skeletal proteins have been discussed earlier on both fusion kinetics [8, 42, 43] and vesiculation

kinetics [3], both of which are fundamental processes that are being increasingly often discussed in the last years [33]. The method used in this study is the phenomenon of the post-fusion oscillation cycle. It was observed and described cursorily in 1987 [17], and could be characterized and explained in detail [3, 5, 7], showing that it serves as a good model for the influence of the cytoskeleton on both the fusion and the vesiculation mechanics within a single model system. The doublet oscillation cycle follows the fusion process and consists of two parts [3]. First, the swell phase, which is characterized by colloid-osmotically driven water uptake into the doublet, observable by a continuing rounding and expansion of the fusion zone diameter. During the swell phase, which lasts between 0.5 sec and more than 180 sec, the membrane area is being stretched. After having reached the maximum tolerated membrane area dilatation of $3.0\% \pm 0.7\%$ [16], the membrane ruptures and ejects intracellular fluid into extracellular space, giving name to the second phase: the pump event. This phase shows an incomplete reverse development of all geometrical parameters within typically 5 msec, giving way to a restart of the cycle. Oscillation cycles can occur from none up to 15 times or more. A similar intracellular fluid jet expulsion from single red blood cells or cell ghosts after membrane rupture has been reported and described earlier [23–25, 44]. It has been shown that the overall mechanical deformability of lysed and resealed red blood cells is virtually identical to that of control cells [34].

This paper extends previous research by introducing a linear elongation modulus Λ that characterizes the fusion zone alone and allows a modelling of the cytoskeleton rearrangements in this area.

Materials and Methods

BLOOD TREATMENT AND CELL FUSION

Human blood was drawn from healthy volunteers by finger prick and diluted in PBS buffer (Life Technologies, Rockville, MD) to match a hematocrit of 2.6%. PBS composition was 0.2 g/l KCl, 0.2 g/l KH_2PO_4 , 8 NaCl and 1.15 g/l Na_2HPO_4 with pH 7.4 and a specific conductivity of 1.321/ Ωm . Samples were stored at $0\text{--}4^\circ\text{C}$ until usage unless otherwise specified. Experiments were carried out not later than $2\frac{1}{4}$ hours after bleeding. For the perfusion heat treatment (HT), which was used to partially denaturate the spectrin network, erythrocytes were exposed by placing 1.0 ml of the cell suspension into a 40°C , 45°C , or 50°C waterbath for 20 minutes before transfer to the microscope. Control cells did not receive the heat treatment but were kept at $0\text{--}4^\circ\text{C}$ until measurement. All experiments were performed in a temperature-controlled observation chamber at $20^\circ\text{C} \pm 0.5^\circ\text{C}$.

The fusion chamber used for these experiments was identical to that described in [3] and allows four experiments with one single chamber assembly. For each experiment, one of the four chambers was filled by dispensing solution from a pipette tip. Two platinum

electrodes (1 mm in width and $100\ \mu\text{m}$ in height with rounded tips) were introduced into the two openings of the chamber and adjusted to a distance of 1 mm.

Erythrocytes in their discocyte shape were allowed to settle on the bottom glass slide to form an almost continuous cell monolayer. A series of three rectangular voltage pulses (amplitude of $800\ \text{V} \pm 20\ \text{V}$, duration of $100\ \mu\text{sec} \pm 2\ \mu\text{sec}$) was applied to the monolayer and thus resulted in an electrical field strength of $8\ \text{kV/cm}$, calculated from an 800-V pulse amplitude divided by the 1 mm electrode spacing. All fusion products were of the ‘open-lumen’ fusion type [38]. The time of membrane and cell fusion was not exactly predictable, it was observed up to 30 sec after the last pulse. Unfused cells showed—depending on the field strength they actually were exposed to—shape changes of varying peculiarity [3, 4, 9], Fig. 1A.

The measurement period lasted from the first pump event up to the fourth pump event, thus covering a total of three swell phases in between. Observation and measurement of cells was done in the middle between both electrodes, because there (i) the change of pH due to electrolytic reasons [27] was expected to be minimal and (ii) the homogeneity of the electrical field distribution had a maximum [3].

IMAGE ACQUISITION AND PARAMETER EXTRACTION

The geometrical shape changes were recorded by a digitally operating CCD-camera MD4256 (Reticon, USA) running at 2 frames per second. The images were recorded into a 2048-images memory buffer installed in a standard PC. Each image had 256×256 pixels with an 8-bit grey-scale resolution. Images were analyzed off-line by an automatic contour extraction algorithm [6], giving for each single image three geometrical values r_1 , r_2 and d_{12} (radius of the bigger sphere, radius of the smaller sphere and distance of the centers of both spheres, respectively), as is defined in Fig. 1B. These values allow the complete calculation of the fusion zone diameter, fusion zone circumference (FZC), membrane area (A) and doublet volume (V) [3]. The images of the camera records provided an optical resolution of $0.42\ \mu\text{m}$. Since the camera images contained optical and thermal noise, the plotted curves of the primary data did not exhibit smooth changes with time (see Fig. 2).

It can be seen in Fig. 2 and has been shown [3], that geometrical changes of the oscillating doublets have a linear characteristic during the swell times between the pump events. Therefore, according to Hooke’s Law, a linear elongation modulus Λ is defined as follows for the fusion zone:

$$\Delta p = \Lambda \cdot \partial FZC \quad (1)$$

where Δp denotes the colloidosmotic pressure difference across the doublet membrane and ∂FZC , the relative change of the fusion zone circumference, which can be accessed via

$$\partial FZC = \frac{FZC_{\text{after}} - FZC_{\text{before}}}{FZC_{\text{before}}} \quad (2)$$

and is equal to the relative change of the fusion zone diameter ∂FZD . The pressure difference Δp itself can be calculated from the formulae of the lateral membrane tension T_{mem} [151, 20] and for the membrane compression modulus K [41], the combination of which results in:

$$\Delta p = \frac{2K}{r} \cdot \partial A \quad (3)$$

where r is the average radius

$$r = \frac{r_1 + r_2}{2} \quad (4)$$

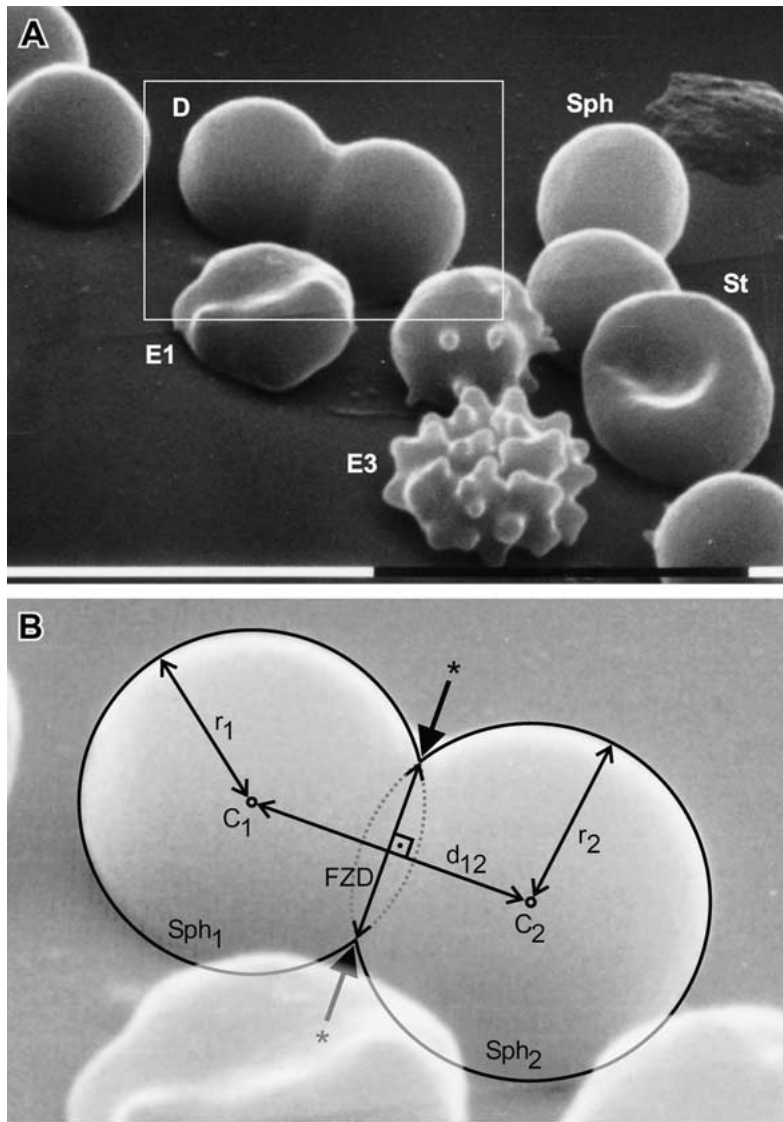


Fig. 1. (A) Scanning electron micrograph of a fused doublet (*D*) in close neighborhood to other unfused erythrocytes of different shapes. Due to the experimental procedure necessary to prepare this image, the cells shown were subject to different electric field strengths, resulting in various cell shapes. Echinocytes I (*E1*) to echinocytes III (*E3*) [10] resulted from shape change after electric field pulses [4, 19], Stomatocytes (*St*) were exposed to negligible electric field strengths and spherocytes (*Sph*) showed colloid osmotic swelling [3] without entering the cell fusion process. The doublet (*D*) shows a smooth contact zone between both spheres, which results from the preparation steps for electron microscopy [6], causing the cell membranes to shrink. This smoothness is at no time observable in light microscopy. The bottom black bar represents a length of 10 μm . (B) Magnification of the white frame from figure A, showing the geometrical parameters of the cell doublet and the definition of the fusion zone. The left sphere (*Sph*₁) with the centerpoint *C*₁ and the radius *r*₁ is connected to the sphere on the right (*Sph*₂) with analogous definitions of centerpoint (*C*₂) and radius (*r*₂). Due to symmetry, the fusion diameter (*FZD*) is always perpendicular to the center point distance *d*₁₂, even if *r*₁ and *r*₂ are unequal. *FZD* is terminated by the intersection points (*) of both spheres.

of the almost spherical doublet at the end of each swell phase (*cf.* respective geometrical dimensions in Fig. 2). ∂A in Eq. (3) is calculated analogously to ∂FZD in Eq. (2).

To further characterize the status of the fusion progress, the doublet roundness (*R*) is calculated by

$$R = \frac{FZD}{d_{12} + r_1 + r_2} \quad (5)$$

where the denominator is identical to the total doublet length. Cells which received the 50°C heat treatment never showed an oscillatory movement, so that results of this study are presented for control cells, 40°C and 45°C HT.

Results and Discussion

An example for a complete oscillation period with 6 pump events of a single doublet is shown in Fig. 2. The almost linear increase of *r*₁, *r*₂ and the linear decrease of *d*₁₂ during the swell phase result in an

increase of membrane area, doublet volume [3], and, which is most important for the characterization of the influence from the spectrin network, the doublet roundness (Fig. 3) and the fusion zone circumference (Fig. 4, where they have been drawn for the first four pump events and swell phases 1 to 3).

OSMOTIC PRESSURE-DIFFERENCE CHANGES

The complete oscillation sequence consists of swell phases and pump events (*see* Fig. 2), which affect periodic changes in the doublet volume and therefore also in the concentration of osmotically active solutes. The necessary equations for their calculation are given in Table 1, where the doublet's initial impermeable solute concentration is taken to be *c*₀. Since every swell phase primarily is characterized by water uptake, the amount of impermeable solute remains

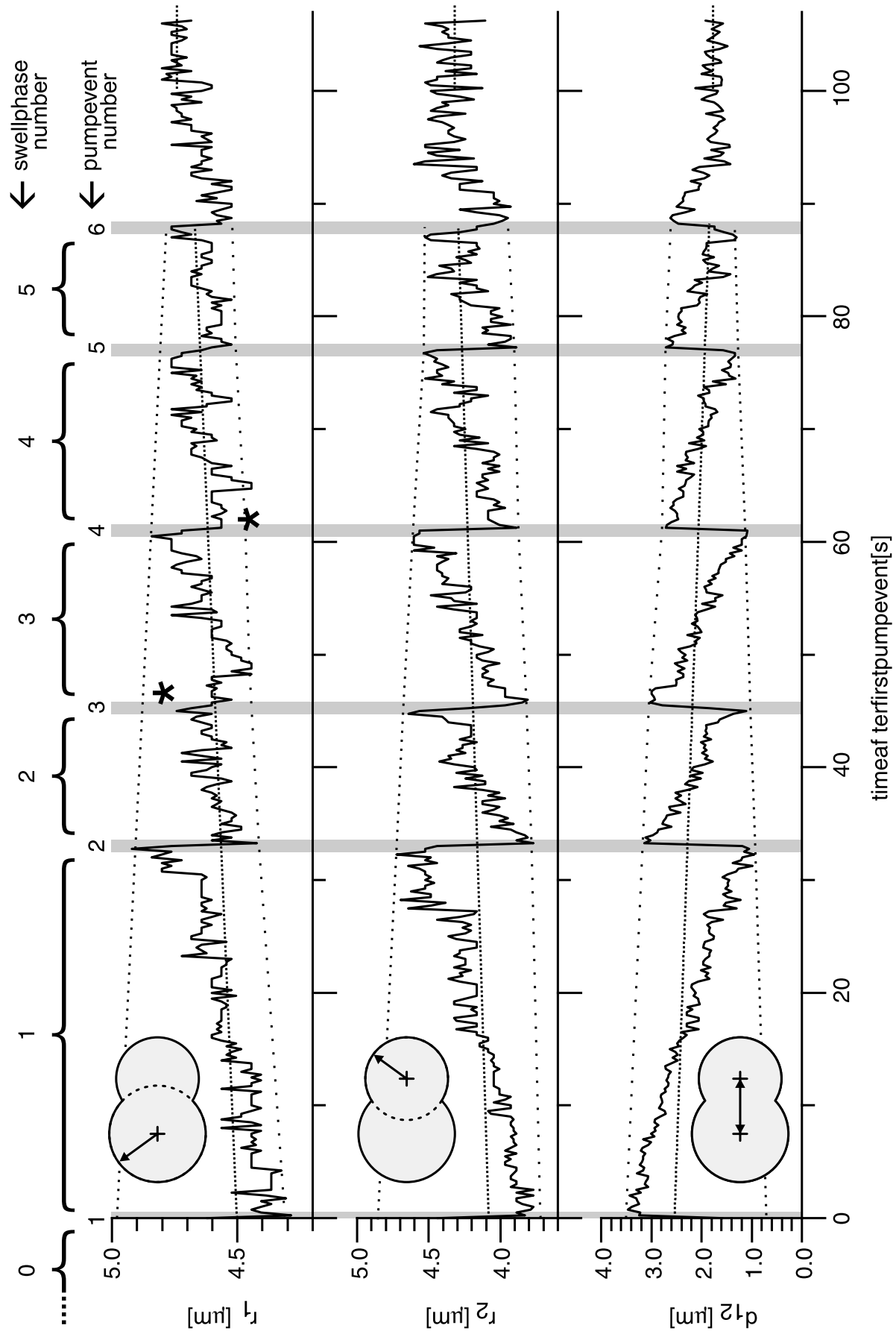


Fig. 2

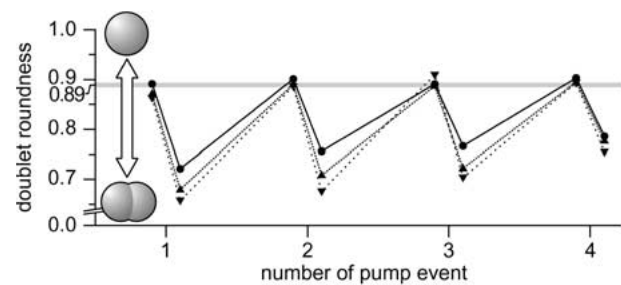


Fig. 3. Roundness values of doublets before and after each of the first four pump events. The linear connections between the marked points serve display purposes and do not reflect linear developments of the respective values. The grey horizontal bar shows the constant average roundness of 0.8901 ± 0.0129 , at which the pump event always starts. Marked points show values for control doublets (●, $N = 14$), 40°C HT (▲, $N = 10$), 45°C HT (▼, $N = 10$). With increasing temperature of the heat treatment, amplitudes of the pre-post-pump event rise, whereas these amplitudes decrease with rising number of pump events. The small insets show the approximate contours of a doublet with the roundness 1 (i.e., a sphere, *top*) and a doublet with the roundness 0.65 (*bottom*).

constant during each individual swell phase, thus decreasing the solute concentration. The development of the doublet volume is a function of consecutive volume increase during the swell phases ($\partial V_s > 0$) and a different volume decrease during the pump events ($\partial V_p < 0$, and $|\partial V_s| > |\partial V_p|$). Therefore, the resulting concentration of osmotically active solutes is constant during each pump event, where endoplasm is ejected into extracellular buffer solution. Due to the very small hematocrit, the extracellular concentration of these solutes practically remains on a constant level. Table 2 gives typical values for the doublet volume and the resulting solute concentration calculated from the equations given in Table 1 and from measured values ∂V_s and ∂V_p . As can be seen from this table, the cluster volume slightly increases with every beginning of a new swell phase, and at the same time the resulting concentration decreases continu-

Fig. 2. Oscillation cycle of a doublet, characterized by the measurement (*solid lines*) of three geometrical parameters (radius of the bigger sphere r_1 , radius of the smaller sphere r_2 and centre distance d_{12}) for 108 sec after the first pump event. Grey vertical bars indicate pump events (fast process, r_1 and r_2 decrease and d_{12} increases) which border the swell phases (slow opposite development of r_1 , r_2 and d_{12}). The narrow dotted lines show the drifting least-square linear fit of the measured curves. *Medium* and *wide dotted lines*: connection of maxima and minima, respectively. The latter two show a, although not linear, unidirectional development towards the point where the oscillation movement ceases, at about 100 sec. The dotted lines starting at 100 sec mark the constant fits after the oscillation has ceased. The asterisks show regions where the measured values do not reach the estimated extreme values, which is caused by noisy images disturbing the automatic contour detection.

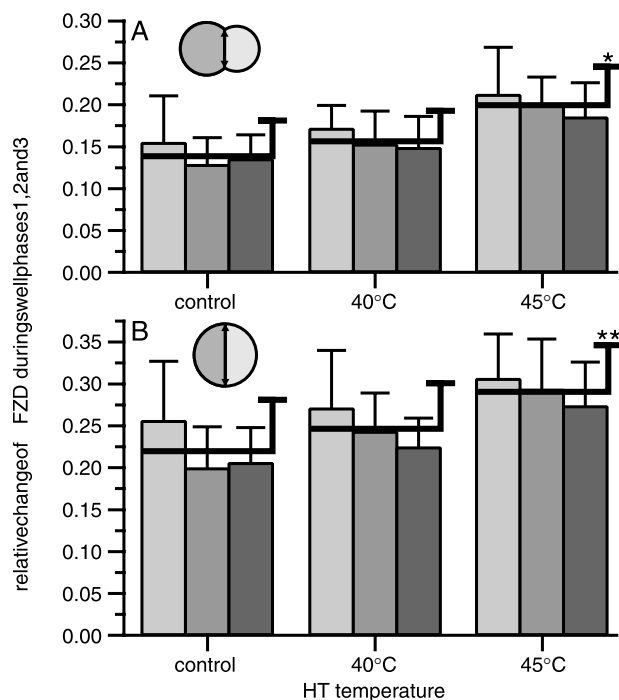


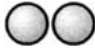





Fig. 4. (A) Relative change of the fusion zone diameter *FZD* and thus equally of the fusion zone circumference *FZC* of doublets during their swell phases 1 to 3 (light, medium and dark grey bars, respectively). Relative changes between the three swell phases do not differ significantly for control or HT and therefore have been combined (thick drawn lines with standard deviations). These are significantly different between control, 40°C HT and 45°C HT (*) at a confidence level $\alpha < 0.01$. (B) Calculated relative changes of fictive doublets not entering the oscillation cycle but ending up in spheres, which can be achieved, e.g., by spectrin denaturation [12]. The relative change of the fusion zone diameter has been calculated such that the membrane area of corresponding doublets A and B is identical. As in A, the combination of swell phases 1 to 3 (thick drawn lines) are significantly different between control, 40°C HT and 45°C HT (**) at a confidence level $\alpha < 0.01$. Also, there is an increase in ∂FZD from measurements (A) to ∂FZD from calculations (B) of 58.3% (control), 57.3% (40°C HT) and 46.5% (45°C HT). (For A and B: $N_{\text{control}} = 14$, $N_{40^\circ\text{C HT}} = 10$, $N_{45^\circ\text{C HT}} = 10$.)

ously and drastically, thus reducing the osmotic force that drives the oscillation speed and amplitude. It has been shown earlier [5], that there is no parallel continuous decreasing trend in the oscillation speed, which allows us to view the development of oscillation parameters not as a function of time, but merely as a function of the ordinal number of the pump events (*see* Figs. 3 and 4).

DRIFTS IN GEOMETRICAL CHANGES

As can be seen in Fig. 2, the amplitudes between the pre- and postfusion geometrical state of r_1 , r_2 and d_{12} decrease unidirectionally and almost linearly, with ongoing oscillation events, although the roundness where the pump event starts is always constant (Fig. 3). This is no contradiction, since

Table 1. Scheme for the calculation of doublet impermeable solutes concentrations

Point of time	Membrane-impermeable solute amount n	Doublet volume V	Resulting concentration $c = n/V$
Pre-fusion 	each sphere $1/2 \cdot n_0$	each sphere $1/2 \cdot V_0$	$\frac{1/2 \cdot n_0}{1/2 \cdot V_0} = \frac{n_0}{V_0} = c_0$
0 th Swell phase start 	n_0	V_0	
0 th Swell phase end 		$(1 + \partial V_{s0}) \cdot V_0$	$\frac{c_0}{(1 + \partial V_{s0})}$
1 st Swell phase start 		$(1 + \partial V_{p1})(1 + \partial V_{s0}) \cdot V_0$	
1 st Swell phase end 	$(1 + \partial V_{p1}) \cdot n_0$	$(1 + \partial V_{s1})(1 + \partial V_{p1})(1 + \partial V_{s0}) \cdot V_0$	$\frac{c_0}{(1 + \partial V_{s1})(1 + \partial V_{s0})}$
2 nd Swell phase start 		$(1 + \partial V_{p2})(1 + \partial V_{s1})(1 + \partial V_{p1})(1 + \partial V_{s0}) \cdot V_0$	
...	$(1 + \partial V_{p1})(1 + \partial V_{p2}) \cdot n_0$...	

The amount of impermeable solute n remains constant from the beginning up end of each swell phase (because of water uptake), whereas the resulting concentration (calculated from n divided by the doublet volume V) is constant during each pump event, i.e., between the end of swell phase i and the beginning of swell phase $i + 1$ (due to the ejection of intracellular liquid into extracellular space). The signed identifier ∂ denotes the relative change of the respective value. According to [3], the swell phase following the cell fusion process is called 0th swell phase, followed by the 1st pump event, 1st swell phase, 2nd pump event and so on.

Table 2. Development of doublet volume and impermeable solutes concentration for the swell phases 1 to 3, starting from 100% at the beginning of the 1st swell phase

Point of time	Beginning of 1 st swell phase	End of 1 st swell phase	Beginning of 2 nd swell phase	End of 2 nd swell phase	Beginning of 3 rd swell phase	End of 3 rd swell phase	...
Doublet volume V	100%	108.6%	101.7%	110.6%	103.8%	112.7%	...
Resulting concentration c	100%	92.1%	92.1%	84.8%	84.8%	78.1%	...

The average volume increase per swell phase is $\partial V_s = 8.6\% \pm 1.6\%$ and the volume decrease per pump event is $\partial V_p = -6.2\% \pm 1.5\%$ with no significant changes between the ordinal number of the swell phases or pump events.

identical values of the roundness can be adopted with different sets of r_1 , r_2 , d_{12} and FZD (Eq. 4). Fig. 2 visualizes the decline of the osmotic pressure difference as has been shown in Table 2. The oscillation ceases during a swell phase, without entering a new pump event.

Fig. 3 shows the doublet roundness values just before and after the pump event number 1 to 4. This figure exhibits that the decrease of the driving osmotic stimulus (Table 2) has no effect on the roundness the doublet adopts when entering a pump event, because it keeps a constant value of 0.8901 ± 0.0129 . Since entering a pump event is identical to

straining of the cell membrane until rupture [3, 5], with the above described observation of the oscillation-time development it can be concluded that at least for the observed first four pump events, the driving osmotic force, although reduced, is always sufficient to stress the membrane to its maximum, irrespective of the degree of the pre-experimental spectrin denaturation for the temperatures examined in this study. Further, there is no influence of the heat treatment on the point where membrane rupture is initiated.

Additionally, Fig. 3 indicates that the geometrical changes during the pump event follow two rules:

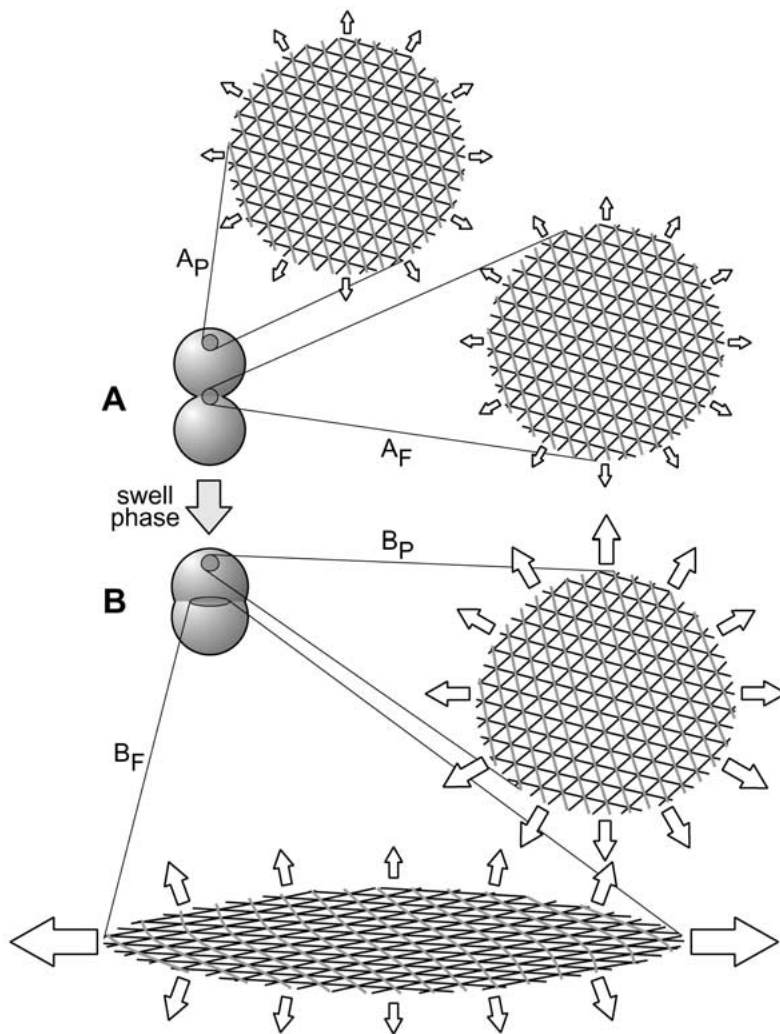


Fig. 5. Triangular spectrin network and the membrane cytoskeleton rearrangement during cell fusion, shown as development of a membrane spot in the fusion zone (subscript “F”) and of a membrane spot close to the doublet pole (subscript “P”). Tangential displacements are induced by tangential forces and are qualitatively shown as white arrows; the arrow size represents the respective magnitude. The displacements and the forces do not alter the topological structure of the triangular mesh, provided the mesh is not torn apart. (A) At the very beginning of the swell phase, both membrane spots, A_P and A_F , are exposed to fully isotropic tangential forces which tend to enlarge the spots’ areas but do not induce deformation. (B) During cell fusion, colloidosmotic forces that elongate the fusion zone (big white arrows, B_F) pull both the phospholipid bilayer and the triangular mesh in the direction of the fusion zone (horizontally), whereas perpendicular to the fusion zone, the resulting forces are much smaller. At the end of the swell phase, the maximum possible area strain of $3.0\% \pm 0.7\%$ [16] has enlarged the area of both spots, B_P and B_F . Whereas spot B_P only suffers from minor deformation, spot B_F has been elongated horizontally. Cytoskeleton components that run in a horizontal direction (black lines) are therefore much more elongated than the perpendicularly oriented components (grey lines).

(i) with ongoing oscillation cycles, the amplitudes decrease for all heat treatments examined and (ii) with increasing temperature of the heat treatment, the amplitudes of the roundness changes become bigger. An increase of this amplitude is caused by a decrease of membrane elasticity. This originates from a partial denaturation of spectrin and the cytoskeleton by the pre-experimental heat treatment.

SPECTRIN REORGANIZATION AND THE LINEAR ELONGATION MODULUS

The constant value of the doublet roundness when entering a pump event gives first evidence of the cytoskeleton rearrangement after membrane fusion. By combining equations 1 to 4, the linear elongation modulus A can be calculated from the measured data given in Fig. 4. For control cells, $A_{\text{control}} = 1.44 \cdot 10^6$ N/m² the value of A decreases with increasing temperature of the heat treatment: $A_{40^\circ\text{C}} = 1.32 \cdot 10^6$ N/m² and $A_{45^\circ\text{C}} = 0.99 \cdot 10^6$ N/m². The spectrin network is assumed to have a triangular structure [11,

30, 39] and through its linkage to membrane proteins it follows partially the bilayer movements during fusion. As Fig. 5 visualizes, the biggest membrane rearrangement takes place in the fusion zone itself. It is characterized by a change in length of the FZC that, when followed by the spectrin triangular network, elongates the network non-isotropically: (i) in the direction of the rim, spectrin is elongated until molecules are almost parallelly stretched and (ii) in the direction perpendicular to the fusion zone, spectrin is not elongated at all, but merely is condensed. Therefore, a further elongation of the fusion zone is almost impossible and the doublet does not achieve the shape of a perfect sphere at the end of the swell phase.

Conclusion

It has been shown earlier that a heat treatment of spectrin accelerates cell fusion kinetics of erythrocytes [42]. This can now be quantified by measurement and calculation of the linear elongation modulus A and

can be explained solely by a rearrangement of the triangular spectrin network and cytoskeleton during the fusion process in the fusion zone, which produces an inhomogeneous cell membrane of the fusion products. Since every pump event is initiated from almost identical values of the doublet roundness, the fusion zone cannot be further expanded without creating a rupture in the cell membrane irrespective of the heat treatment. Membranes of other cell types with a spectrin network will show similar behavior, but with different values for the linear elongation modulus.

The expert technical assistance of Rosa Maria Degenhardt is gratefully acknowledged.

References

- Ahkong, Q., Lucy, J.A. 1988. Localized osmotic swelling and cell fusion in erythrocytes: possible implications for exocytosis. *J. Cell. Sci.* **91**:597–601
- Akkas, N. 1984. Biomechanics of virus-to-cell and cell-to-cell fusion. *J. Biomed. Eng.* **6**:257–264
- Baumann, M. 1999. Dynamics of oscillating erythrocyte doublets after electrofusion. *Biophys. J.* **77**:2602–2611
- Baumann, M. 2001. Early stage shape change of human erythrocytes after application of electric field pulses. *Mol. Membr. Biol.* **18**: 153–160
- Baumann, M., Grebe, R. 1998. Characteristics of the osmotically induced membrane rupture. *Mol. Membr. Biol.* **15**:193–201
- Baumann, M., Grebe, R. 2000. Automated surface and volume measurement of fused cells. *Anal. Quant. Cytol. Histol.* **22**:247–257
- Baumann, M., Sowers, A.E. 1996. A mechanical cycling phenomenon in electrofused erythrocytes. *Mol. Membr. Biol.* **13**:113–119
- Baumann, M., Sowers, A.E. 1996. Membrane skeleton involvement in cell fusion kinetics: A parameter that correlates with erythrocyte osmotic fragility. *Biophys. J.* **71**:336–340
- Bennett, V. 1990. Spectrin based membrane skeleton: a multipotential adaptor between plasma membrane and cytoplasm. *Physiol. Rev.* **70**:1029–1065
- Bessis, P.M. 1977. Erythrocyte form and deformability for normal blood and some hereditary hemolytic anaemias. *Nouv. Rev. Hemat.* **18**:75–94
- Boal, D.H. 1994. Computer simulation of a model network for the erythrocyte cytoskeleton. *Biophys. J.* **71**:336–340
- Chernomordik L.V., Sowers, A.E. 1991. Evidence that the spectrin network and a nonosmotic force control the fusion product morphology in electrofused erythrocyte ghosts. *Biophys. J.* **60**:1026–1037
- de Arcuri, B.F., Vechetti, G.F., Chehin, R.N., Goñi, F.M., Moore, R. D. 1999. Protein-induced fusion of phospholipid vesicles of heterogeneous sizes. *Biochem. Biophys. Res. Commun.* **262**:586–590
- Dimitrov, D.S., Apostolova, M.A., Sowers, A.E. 1990. Attraction, deformation and contact of membranes induced by low frequency electric fields. *Biochim. Biophys. Acta* **1023**:389–397
- Evans, E.A., Waugh, R. 1977. Osmotic correction to elastic area compressibility measurements on red cell membrane. *Biophys. J.* **20**:307–313
- Evans, E.A., Waugh, R., Melnik, L. 1976. Elastic area compressibility modulus of red cell membrane. *Biophys. J.* **16**:585–595
- Glaser, R.W., Donath, E. 1987. Hindrance of red cell electrofusion by the cytoskeleton. *Studia Biophysica* **121**: 37–43
- Häussinger, D., Schliess, F. 1999. Osmotic induction of signalling cascades: Role in regulation of cell function. *Biochem. Biophys. Res. Commun.* **255**:551–555
- Henszen, M.M.M., Weske, M., Schwarz, S., Haest, C.W.M., Deuticke, B. 1997. Electric field pulses induce reversible shape transformation of human erythrocytes. *Mol. Membr. Biol.* **14**: 195–204
- Jay, A.W.L., Canham, P.B. 1977. Viscoelastic properties of the human red blood cell membrane. II. Area and volume of individual red cells entering a micropipette. *Biophys. J.* **17**:169–178
- Knutton, S., Pasternak, C.A. 1979. The mechanism of cell-cell fusion. *Trends Biochem. Sci.* **4**:220–223
- Köhler, G., Milstein, C. 1975. Continuous culture of fused cells secreting antibody of predefined specificity. *Nature* **256**:495–497
- Lieber, M.R., Steck, T.L. 1982. A description of the holes in human erythrocyte membrane ghosts. *J. Biol. Chem.* **257**: 11651–11659
- Lieber, M.R., Steck, T.L. 1982. Dynamics of the holes in human erythrocyte membrane ghosts. *J. Biol. Chem.* **257**:11660–11666
- Marsden N.V., Zade-Oppen A.M., Davies HG. 1981. Jet expulsion of cellular contents from rad cells during photodynamic hemolysis. *Ups. J. Med. Sci.* **86**:1–8
- Morris, S.J., Sarkar, D.P., White, J.M., Blumenthal, R. 1989. Kinetics of pH dependent fusion between 3T3 fibroblasts and expressing influenza hemagglutinin and red blood cells: Measurement by quenching of fluorescence. *J. Biol. Chem.* **264**:3972–3978
- Potter, H. 1988. Electroporation in biology: Methods, application and instrumentation. *Anal. Biochem.* **174**:361–373
- Prüfer, D., Kawchuk, L., Monecke, M., Nowok, S., Fischer, R., Rohde, W. 1999. Immunological analysis of potato leafroll luteovirus (PLRV) P1 expression identifies a 25kDa RNA-binding protein derived via P1 processing. *Nucl. Acids Res.* **27**:421–425
- Rauch, C., Farege, E. 2000. Endocytosis switch controlled by transmembrane osmotic pressure and phospholipid number asymmetry. *Biophys. J.* **78**:3036–3047
- Saxton, M.J. 1990. The membrane skeleton of erythrocytes. A percolation model. *Biophys. J.* **57**:1167–1177
- Schmid-Schönbein, H., Heidtmann, H., Grebe, R. 1986. Spectrin, red cell shape and deformability: I. Membrane curvature in genetic spectrin deficiency. *Blut* **52**:131–147
- Schmid-Schönbein, H., Heidtmann, H., Grebe, R. 1986. Spectrin, red cell shape and deformability: II. The antagonistic action of spectrin and sialic acid residues in determining membrane curvature in genetic spectrin deficiency in mice. *Blut* **52**:149–164
- Schneider, S.W. 2001. Kiss and run mechanism in exocytosis. *J. Membrane Biol.* **181**:67–76
- Scott, M.D., Kuypers, F.A., Butikofer, P. Bookchin, R.M., Ortiz, O.E., Lubin, B.H. 1990. Effect of osmotic lysis and re-sealing on red cell structure and function. *J. Lab. Clin. Med.* **115**:470–480
- Song, L., Ahkong, Q.F., Georgescauld, D., Lucy, J.A. 1991. Membrane fusion without cytoplasmic fusion (hemi-fusion) in erythrocytes that are subjected to electrical breakdown. *Biochim. Biophys. Acta* **1065**:54–62
- Sowers, A.E. 1992 The role of both postfusion expansion and membrane fusion in the entry of cells by enveloped viruses. *In*

- Advances in membrane fluidity, membrane interactions of HIV: Implication for pathogenesis and therapy in AIDS (Aloia R.C., and Curtain, C., Eds.), pp 203–214, Wiley-Liss, New York
37. Sowers, A.E. 1995. Membrane skeleton restraint of surface shape change during fusion of erythrocyte membranes: evidence from use of osmotic and dielectrophoretic microforces as probes. *Biophys. J.* **69**:2507–2516
 38. Sowers, A. E., Rosenberg, J.D., Yankuan, W. 1994. Discovery of new structure-function relationships in the erythrocyte spectrin-based A. membrane skeleton: A study using electrofused ghost membranes. *In* Charge and field effects. Allen, M.J., Cleary, S.F., and Sowers, A.E., Eds., pp 403–419, World Scientific Publishing Co
 39. Steck, T.L. 1989. Red cell shape. *In*: Cell shape: determinants, regulation and regulatory role. Stein, W., Bronner, F., Eds., pp. 205–246, Academic Press, New York
 40. Steubing, R.W., Cheng, S., Wright, W.H., Numajiri, Y., Berns, M.W. 1994. Laser induced cell fusion in combination with optical tweezers: The laser cell fusion trap. *Cytometry* **12**:505–510
 41. Waugh, R., Evans, E.A. 1979. Thermoelasticity of red blood cell membrane. *Biophys. J.* **26**:115–132
 42. Wu, Y.-K., Rosenberg, J.D., Sowers, A.E. 1994. Surface shape change during fusion of erythrocyte membranes is sensitive to membrane skeleton agents. *Biophys. J.* **67**:1896–1905
 43. Wu, Y.-K., Sjodin, R.A., Sowers, A.E. 1994. Distinct mechanical relaxation components in pairs of erythrocyte ghosts undergoing fusion. *Biophys. J.* **66**:114–119
 44. Zade-Oppen, A.M. 1998. Repetitive cell 'jumps' hypotonic lysis of erythrocytes observed with a simple flow chamber. *J. Microsc.* **192**:54–62
 45. Zimmerman, U., Vienken, J. 1982. Electric field induced cell-to-cell fusion. *J. Membrane Biol.* **67**:165–182